IMPROVEMENT ON SIX-NODE TRIANGULAR FINITE ELEMENT (IT6) USING TWICE-INTERPOLATION STRATEGY FOR LINEAR ELASTIC FRACTURE MECHANICS

Hoang Lan-Ton That[1,2], Thanh Chau-Dinh[1], Hieu Nguyen-Van[2]
[1]*Ho Chi Minh City University of Technology and Education, Viet Nam.*
[2]*Ho Chi Minh City University of Architecture, Viet Nam.*

Received 18/7/2018, Peer reviewed 1/10/2018, Accepted for publication 10/10/2018

ABSTRACT

An improved six-node triangular finite element based on a twice-interpolation strategy (TIS) for accurately modeling singular stress fields near crack tips of two-dimensional (2D) cracks in solids is presented. In contrast to the traditional approaches, the approximation functions constructed based on the TIS involve both nodal values and averaged nodal gradients. The main idea of applying the TIS is to make the trial solution and its derivatives continuous across inter-element boundaries, or in other words, stresses can be smoothly transited element by element. This could improve the accuracy of the computed gradients of the trial solution and avoid tackling the smoothing operation technique generally utilized during the post-processing process. Another important issue should be noted that the TIS does not increase the total number of the degrees of freedom (DOFs) of the whole system. It implies that the total number of DOFs discretized by the proposed element is the same as that by the standard FEM. The stress intensity factors (SIFs) are estimated using the proposed method. The accuracy and efficiency of the proposed element are verified by some numerical examples.

Keywords: *Twice-interpolation strategy (TIS); six-node triangular element; stress intensity factors (SIFs); linear elastic fracture mechanic; edge-cracked plate; three-point bending beam.*

1. INTRODUCTION

Numerical modeling of the stress fields near a crack tip remains a challenging problem in the scientific community of computational fracture mechanics. The accurate predictions of the singular stress fields near the crack tip play a crucial role in maintenance, life prediction and safety assessment of advanced engineering materials and structures. Many approaches including analytical, semi-analytical, experimental, numerical methods have been introduced and developed for fracture modeling over the past few decades. In terms of the numerical approaches, the finite element method (FEM) is a powerful tool as it has been extensively used for solving a variety of engineering problems. By using special elements such as singular crack-tip elements [1], enriched elements [2], etc., the FEM can be applied for extracting the stress intensity factors. In addition, a smoothing operation employed for stresses recovery at the post-processing state is often required by the FEM. Therefore, many efforts have been put forward to the developments of new or improved numerical techniques to facilitate or overcome the difficulties in the classical methods, for example, the extended finite element method (XFEM) [3], meshfree methods and coupled FE-EFG method [4], smoothed FEM [5], extended isogeometric analysis [6], just to name a few. Although the FEM has successfully been applied to a wide range of engineering problems in many fields, it is well-known that the gradients of field variables given by the FEM are discontinuous among internal element edges. Such discontinuity also happens at the nodes. In practice, an extra task pertaining to the smoothing operation to the nodal stress in

the post-processing procedure is often required. In recent years, Zheng et al. [7] presented an improved triangular element for elastostatic problems in which the new concept of the TIS acting on the interpolation functions is proposed. The new triangular element is very attractive as it owns various desirable features that are not available in the standard elements. The proposed element shows that the stresses at nodes are not only continuous without the need for the smoothing operation but also more accurate than that derived from the standard triangular element. The main idea behind the method comes up with the approximation functions based on the TIS. Basically, the approximation functions handle both the nodal values and the averaged nodal gradients as interpolation conditions, see Zheng et al. [7] for details. Nevertheless, the major motivation of applying the TIS is to make the trial solution and its derivatives continuous across inter-element boundaries, or in other words, stresses in the domain can be smoothly transited element by element. This could improve the accuracy of the computed gradients of the trial solution and avoid tackling the smoothing operation technique generally utilized during the post-processing process. Another important issue should be noted that the TIS does not increase the total number of the degrees of freedom (DOFs) of the whole system. It implies that the total number of DOFs discretized by the proposed element is the same as that by the standard FEM.

The main objective of this paper is to improve the six-node triangular finite element based on TIS for accurately modeling singular stress fields near crack tips of two-dimensional (2D) cracks in solids. The stress intensity factors (SIFs) calculated by the proposed element are validated against reference solutions. The body of the paper is organized into five Sections. In Section 2, formulation of this new element (IT6) for 2D cracked problems is derived in which the construction of the shape functions and their properties are presented. The small modification of IT6 becomes singular IT6 around crack tip and the calculation of SIFs is described in Section 3. The numerical examples are subsequently presented in Section 4. We end with conclusions in the last Section.

2. FORMULATION OF IT6

In this section, the construction of the IT6 shape functions and their properties are briefly given. Let $\mathbf{x} = (x, y)$ be a point in a six-node triangular element with nodes i, j, k, m, n, p as schematically sketched in Fig.1a. We here denote by S_{imp}, S_{jmn} and S_{knp} support domains that are also shown in Fig.1a, respectively. The supporting nodes for the point $\mathbf{x}$ in the IT6 element involve all nodes of support domains S_{imp}, S_{jmn} and S_{knp}. The IT6 support domain for point $\mathbf{x}$ is much larger than the standard FEM support domain, and the trial solution at point $\mathbf{x}$ can be written as

$$u^h(x) = \sum_{l=1}^{n_{sp}} \tilde{N}_l(\mathbf{x}) d_l = \tilde{\mathbf{N}}(\mathbf{x})\mathbf{d} \tag{1}$$

In Eq. (1), the twice-interpolation shape function $\tilde{N}_l$ is determined

$$\begin{aligned}\tilde{N}_l = &\underbrace{\phi_i N_l^{[i]} + \phi_{ix}\bar{N}_{l,x}^{[i]} + \phi_{iy}\bar{N}_{l,y}^{[i]}}_{\text{node } i} + \underbrace{\phi_j N_l^{[j]} + \phi_{jx}\bar{N}_{l,x}^{[j]} + \phi_{jy}\bar{N}_{l,y}^{[j]}}_{\text{node } j} \\ &+ \underbrace{\phi_k N_l^{[k]} + \phi_{kx}\bar{N}_{l,x}^{[k]} + \phi_{ky}\bar{N}_{l,y}^{[k]}}_{\text{node } k} + \underbrace{\phi_m N_l^{[m]} + \phi_{mx}\bar{N}_{l,x}^{[m]} + \phi_{my}\bar{N}_{l,y}^{[m]}}_{\text{node } m} \\ &+ \underbrace{\phi_n N_l^{[n]} + \phi_{nx}\bar{N}_{l,x}^{[n]} + \phi_{ny}\bar{N}_{l,y}^{[n]}}_{\text{node } n} + \underbrace{\phi_p N_l^{[p]} + \phi_{px}\bar{N}_{l,x}^{[p]} + \phi_{py}\bar{N}_{l,y}^{[p]}}_{\text{node } p}\end{aligned} \tag{2}$$

where d_l denotes the nodal displacement vector, while $N_l^{[i]}$ is the shape function with respect to node *i*, and n_{sp} is the total number of the supporting nodes in regard to the point of interest **x**. In the following interpretation, the formulation of the average derivative of the shape functions at node *i* is given (similar for other nodes).

$$\bar{N}_{l,x}^{[i]} = \sum_{e \in S_{imp}} \left(\omega_e N_{l,x}^{[i][e]} \right); \quad \bar{N}_{l,y}^{[i]} = \sum_{e \in S_{imp}} \left(\omega_e N_{l,y}^{[i][e]} \right) \tag{3}$$

In Eq. (3), the term $N_{l,x}^{[i][e]}$ is the derivative of $N_l^{[i]}$ computed in element *e*, and ω_e is the weight function of element $e \in S_{imp}$, which is defined by

$$\omega_e = \frac{\Delta_e}{\sum_{\tilde{e} \in S_{imp}} \Delta_{\tilde{e}}} \quad \text{with} \quad e \in S_{imp} \tag{4}$$

with Δ_e being the area of the element *e*. In Eq. (2), the functions ϕ_i, ϕ_{ix} and ϕ_{iy} forming the polynomial basis associated with node *i* must satisfy the following conditions

$$\begin{gathered} \phi_i(\mathbf{x}_l) = \delta_{il}, \ \phi_{i,x}(\mathbf{x}_l) = 0, \ \phi_{i,y}(\mathbf{x}_l) = 0 \\ \phi_{ix}(\mathbf{x}_l) = 0, \ \phi_{ix,x}(\mathbf{x}_l) = \delta_{il}, \\ \phi_{ix,y}(\mathbf{x}_l) = 0 \\ \phi_{iy}(\mathbf{x}_l) = 0, \ \phi_{iy,x}(\mathbf{x}_l) = 0, \\ \phi_{iy,y}(\mathbf{x}_l) = \delta_{il} \end{gathered} \tag{5}$$

where *l* is any one of the indices *i*, *j*, *k*, *m*, *n* and *p*, and

$$\delta_{il} = \begin{cases} 1 & if \quad i = l \\ 0 & if \quad i \neq l \end{cases} \tag{6}$$

We also note that the above conditions have to be applied in a similar manner to other functions, i.e., ϕ_j, ϕ_{jx}, ϕ_{jy}, ϕ_k, ϕ_{kx}, ϕ_{ky}, ϕ_m, ϕ_{mx}, ϕ_{my}, ϕ_n, ϕ_{nx}, ϕ_{ny}, ϕ_p, ϕ_{px}, and ϕ_{py}. These polynomial basis functions ϕ_i, ϕ_{ix} and ϕ_{iy} for the IT6 element are given by (7)

$$\begin{aligned} \phi_i &= L_i + L_i^2 L_j + L_i^2 L_k + L_i^2 L_m + L_i^2 L_n + L_i^2 L_p \\ &\quad - L_i L_j^2 - L_i L_k^2 - L_i L_m^2 - L_i L_n^2 - L_i L_p^2 \\ \phi_{ix} &= -(x_i - x_j)\left(L_i^2 L_j + 0.5 L_i L_j L_k + 0.5 L_i L_j L_m + 0.5 L_i L_j L_n + 0.5 L_i L_j L_p\right) \\ &\quad - (x_i - x_k)\left(L_i^2 L_k + 0.5 L_i L_k L_j + 0.5 L_i L_k L_m + 0.5 L_i L_k L_n + 0.5 L_i L_k L_p\right) \\ &\quad - (x_i - x_m)\left(L_i^2 L_m + 0.5 L_i L_m L_j + 0.5 L_i L_m L_k + 0.5 L_i L_m L_n + 0.5 L_i L_m L_p\right) \\ &\quad - (x_i - x_n)\left(L_i^2 L_n + 0.5 L_i L_n L_j + 0.5 L_i L_n L_k + 0.5 L_i L_n L_m + 0.5 L_i L_n L_p\right) \\ &\quad - (x_i - x_p)\left(L_i^2 L_p + 0.5 L_i L_p L_j + 0.5 L_i L_p L_k + 0.5 L_i L_p L_m + 0.5 L_i L_p L_n\right) \\ \phi_{iy} &= -(y_i - y_j)\left(L_i^2 L_j + 0.5 L_i L_j L_k + 0.5 L_i L_j L_m + 0.5 L_i L_j L_n + 0.5 L_i L_j L_p\right) \\ &\quad - (y_i - y_k)\left(L_i^2 L_k + 0.5 L_i L_k L_j + 0.5 L_i L_k L_m + 0.5 L_i L_k L_n + 0.5 L_i L_k L_p\right) \\ &\quad - (y_i - y_m)\left(L_i^2 L_m + 0.5 L_i L_m L_j + 0.5 L_i L_m L_k + 0.5 L_i L_m L_n + 0.5 L_i L_m L_p\right) \\ &\quad - (y_i - y_n)\left(L_i^2 L_n + 0.5 L_i L_n L_j + 0.5 L_i L_n L_k + 0.5 L_i L_n L_m + 0.5 L_i L_n L_p\right) \\ &\quad - (y_i - y_p)\left(L_i^2 L_p + 0.5 L_i L_p L_j + 0.5 L_i L_p L_k + 0.5 L_i L_p L_m + 0.5 L_i L_p L_n\right) \end{aligned} \tag{7}$$

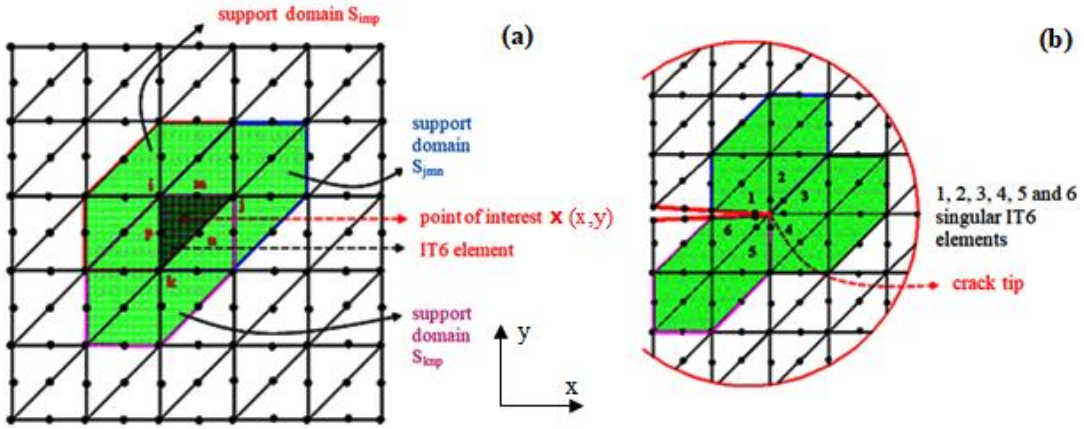

Figure 1. ***(a)*** *Six-node triangular element and its support domain.* ***(b)*** *Illustration of the support domains around crack tip.*

Other functions can be also calculated in the same manner by a circulatory permutation of indices *i, j, k, m, n* and *p*. In addition, L_i, L_j, L_k, L_m, L_n and L_p are the area coordinates of the point of interest **x** in the six-node triangular element *i, j, k, m, n, p*, see [7] for more details. These shape functions are complete polynomials, satisfy properties of the partition of unity, and possess Kronecker's delta function property.

The element stiffness matrix $\mathbf{K_e}$ can be finally expressed as

$$\mathbf{K}_e = \int_{\Omega_e} \tilde{\mathbf{B}}_e^T \mathbf{D} \tilde{\mathbf{B}}_e \mathrm{d}\Omega \tag{8}$$

with **D** is elastic tensor and

$$\tilde{\mathbf{B}}_e = \begin{bmatrix} \tilde{N}_{1,x} & 0 & \tilde{N}_{2,x} & 0 & \dots & \tilde{N}_{l,x} & 0 & \dots & \tilde{N}_{n_{sp},x} & 0 \\ 0 & \tilde{N}_{1,y} & 0 & \tilde{N}_{2,y} & \dots & 0 & \tilde{N}_{l,y} & \dots & 0 & \tilde{N}_{n_{sp},y} \\ \tilde{N}_{1,y} & \tilde{N}_{1,x} & \tilde{N}_{2,y} & \tilde{N}_{2,x} & \dots & \tilde{N}_{l,y} & \tilde{N}_{l,x} & \dots & \tilde{N}_{n_{sp},y} & \tilde{N}_{n_{sp},x} \end{bmatrix}_{3\times 2n_{sp}} \tag{9}$$

n_{sp} is the total number of the supporting nodes in regard to the point of interest.

3. MODIFIED IT6 AROUND CRACK TIP

In the mid-1970s, Barsoum [8], Henshell and Shaw [9] independently discovered that by taking the midside nodes of an element that is adjacent to a crack tip and moving them to the quarter-point of the element side, the singular stress field which occurs at a crack tip could be produced. This was a significant discovery since researchers had spent great efforts trying to develop special elements which could capture this behavior. The fact has proved that the quarter-point element (QPE) may be used in any finite element code makes it extremely valuable.

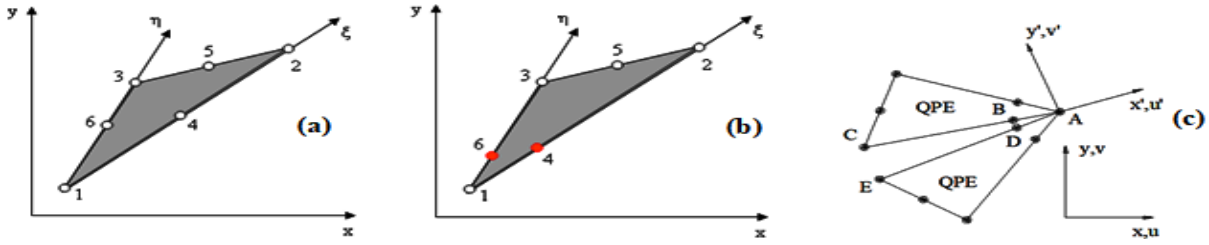

Figure 2. *Six-node triangular elements:* ***(a)*** *with midside nodes,* ***(b)*** *with quarter-point nodes,* ***(c)*** *nodal lettering for stress intensity computation.*

In this paper, we use quarter-point techniques to modify the six-node triangular element with midside nodes as shown in Fig.2a to six-node triangular element with quart-point nodes (node 4 and node 6) as shown in Fig.2b if node 1 is considered as crack tip point. The support domains around crack tip are also presented in Fig.1b. The SIFs are directly evaluated from

$$K_I = \frac{G}{K+1}\sqrt{\left(\frac{2\pi}{L}\right)\left\{4\left(v_B^{'}-v_D^{'}\right)-\left(v_C^{'}-v_E^{'}\right)\right\}}$$
$$K_{II} = \frac{G}{K+1}\sqrt{\left(\frac{2\pi}{L}\right)\left\{4\left(u_B^{'}-u_D^{'}\right)-\left(u_C^{'}-u_E^{'}\right)\right\}} \quad (10)$$

where G is the shear modulus, K is 3-4ν for plane strain and (3-ν)/(1+ν) for plane stress, ν is the Poisson's ratio, L is QPE length along crack face, and u', v' are local displacement along and normal to crack face as depicted in Fig.2c.

4. NUMERICAL RESULTS

In this section, we will verify the accuracy of the IT6 element through some 2D-cracked problems.

4.1 The edge-cracked plate under tensile load

The first example deals with a finite rectangular plate with an edge crack either subjected to a uniform tensile load on the top of the plate. The geometry of the plate is schematically depicted in Fig.3a. The bottom edge of the plate is fully clamped. The dimensionless geometric parameters for the plate are set up as follows: the length of the plate L = 16, the width W = 7, and a crack length a = W/2.

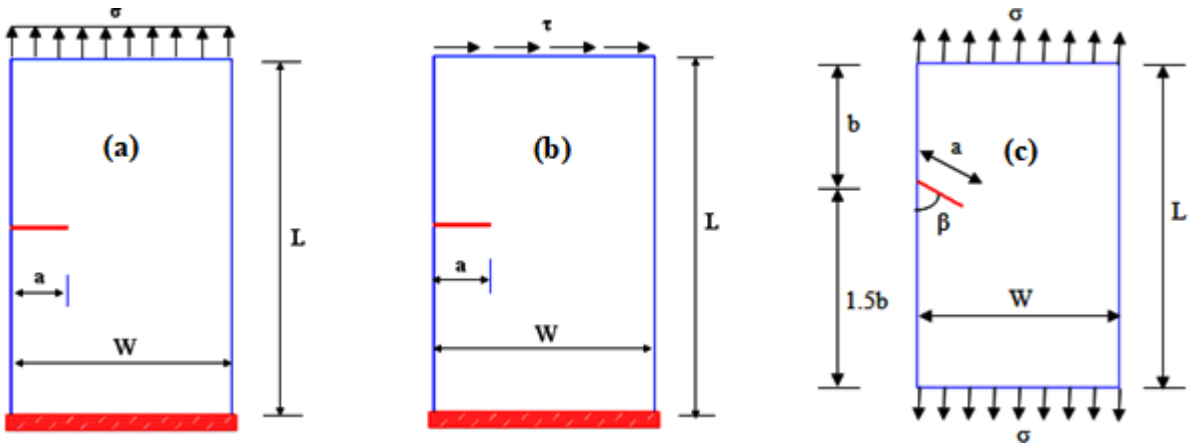

Figure 3. *Geometry of edge-cracked plates under* ***(a)*** *tensile load,* ***(b)*** *shear load and* ***(c)*** *slant edge-cracked plate under tension.*

Table 1. *The convergence of the SIFs for an edge-cracked plate under tensile load.*

	Mesh	T6	IT6	Reference result [10]
K_I	9x9	8.4026	9.2321	**9.3738**
		(10.36%)	*(1.51%)*	
	13x13	8.8532	9.3664	
		(5.55%)	*(0.08%)*	

The plate is subjected to the normal stress σ = 1 on the top of the plate, and under such condition the only mode I can develop. The numerical mode-I SIF is compared with

the analytical solutions given by Ewalds and Wanhill [10] $K_I = C\sigma\sqrt{\pi a}$, where C is determined by

$$C = 1.12 - 0.231\left(\frac{a}{W}\right) + 10.55\left(\frac{a}{W}\right)^2 - 21.72\left(\frac{a}{W}\right)^3 + 30.39\left(\frac{a}{W}\right)^4 \quad (11)$$

The numerical results of mode-I SIF given by the IT6 and T6 elements are presented in Table.1. As compared with the reference results [10], the SIFs provided by the IT6 elements are more accurate than those of the conventional T6. To exhibit the performance of IT6 in stress distribution, we plot the σ_x stress contour with regular mesh size 45x45 elements in Fig.4.

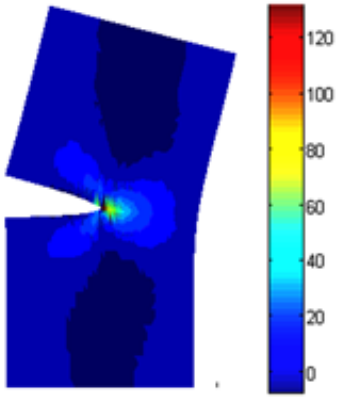

Figure 4. *Stress field under tensile load*

4.2 An edge-cracked plate under shear load

This example deals with a finite rectangular plate with an edge cracks subjected to a uniform shear load on the top of the plate. The geometry of the plate is illustrated in Fig.3b. The bottom edge of the plate is fully clamped. The dimensionless geometric parameters for this plate are also set up as follows: the length of the plate L = 16, the width W = 7, and a crack length a = $W/2$. A shear load τ = 1 subjected to the top of the plate is considered. This is a mixed mode problem. The exact solutions of the mixed-mode SIFs for this case of shear loading condition [3], K_I = 34.0 and K_{II} = 4.55, are used for the comparison purpose. Once again, the numerical results presented in Table.2 show that the IT6 elements can give SIFs of both modes I and II more accurately than those given by the conventional T6 elements.

Table 2. *The Convergence of the SIFs for an edge-cracked plate under shear load.*

	Mesh	T6	IT6	Reference results [3]
K_I	13x13	33.2206	32.8085	**34**
		(2.29%)	*(3.50%)*	
	17x17	33.9243	33.9463	
		(0.22%)	*(0.16%)*	
	Mesh	T6	IT6	Exact result
K_{II}	13x13	3.3091	4.4883	**4.55**
		(27.27%)	*(1.35%)*	
	17x17	3.4863	4.5376	
		(23.38%)	*(0.27%)*	

4.3 A slant edge-cracked plate under tension

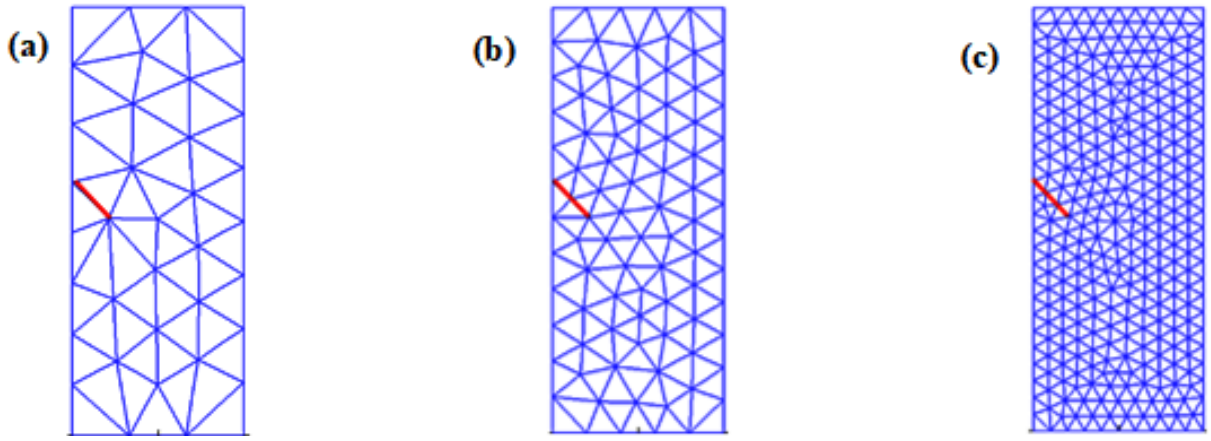

Figure 5. *Mesh for plate with slant edge crack in case a/W = 0.3*
(a) *52 elements,* ***(b)*** *147 elements and* ***(c)*** *566 elements for convergence.*

A rectangular plate is shown in Fig.3c with the dimensions of L = 2.5 cm and $b = W$ = 1.0 cm. An oblique edge crack of length a is in plate with $\beta = 67.5^{o}$. Material properties of the plate are E = 190GPa, ν = 0.25. The stress intensity factors of the crack tip K_I and K_{II} are calculated with 566 IT6 elements as shown in Fig.5c while the plate is subjected to uniform tension on the ends. The analytical solution of this model is given as

$$K_I = F_I \sigma\sqrt{\pi a} \qquad K_{II} = F_{II}\sigma\sqrt{\pi a} \qquad \Rightarrow \qquad F_i = \frac{K_i}{\sigma\sqrt{\pi a}} \qquad with \qquad i = I, II \tag{12}$$

Fig.6 shows the normalized stress intensity factors (F_I, F_{II}) given by the IT6 elements and the boundary element method [11]. As demonstrated in the figure, the IT6 elements can give results in good agreement with the reference.

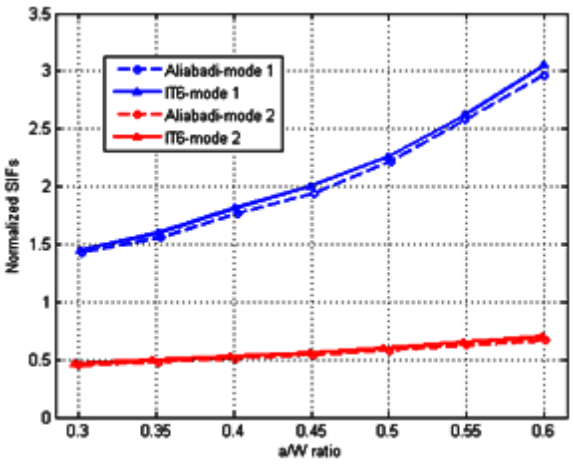

Figure 6. *Normalized SIFs (F_I, F_{II})*

4.4 A three-point bending beam containing an edge crack

Finally, let us consider a three-point bending beam (TPB) containing an edge crack of length a as depicted in Fig.7a. The geometric parameters of the TPB are set to be W = 6 and L = 12. The beam is subjected to a concentrated force specified by F = 1, while the edge crack is assumed to locate at the mid-span of the TPB beam. As a result, the beam has only mode-I SIF. The analytical solution with crack length $a = 0.3W$ is given by Srawley [12, 13]. Other reference solution is also provided based on the PUM [14]. Table 3 compares the numerical result calculated by the IT6 element, the PUM and the analytical method. Table.3 and Fig.7b demonstrate the convergence of the mode-I SIF given by the IT6 elements to the analytical solution [12, 13] .

Table 3. *Convergence of the SIFs for an edge-cracked on a three-point bending beam.*

	Mesh	IT6	PUM	Exact result
K_I (a/W = 0.3)	33x21	2.2268		
	37x21	2.3113		
	41x21	2.3750	2.514	**2.484**
	45x21	2.4240		
	49x21	2.4622		

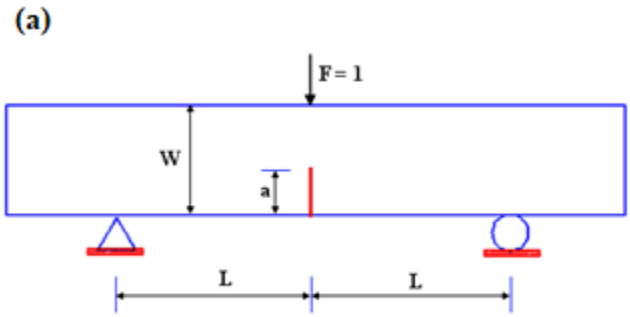

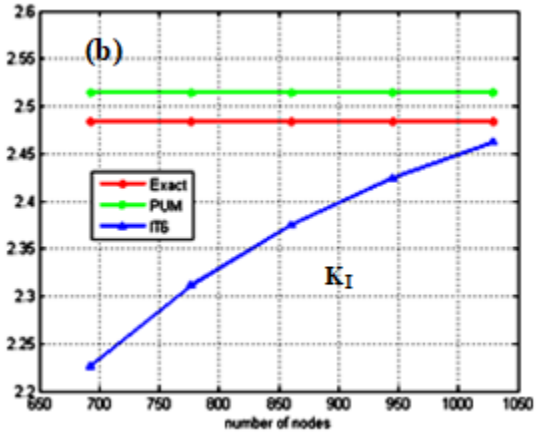

Figure 7. (a) *Geometry of a TPB beam* ***(b)*** *K_I for TPB beam with an edge crack.*

5. CONCLUSIONS

The six-node triangular element IT6 has been developed for accurately computing the SIFs of 2D-cracked problems. The IT6 element has been used to analyze the SIFs of some benchmark linear elastic fracture mechanics problems in 2D. The numerical results of the SIFs provided by the IT6 elements agree well with the analytical results, or other numerical methods. The proposed IT6 elements perform more accurately than the conventional T6 elements in all numerical examples. Although the computational time of the whole procedure based on the TIS elements is higher than those based on the conventional elements due to the TIS procedure, the IT6 elements also more efficient in term of the accuracy and the need for not using a post-processing of any smoothing operation.

REFERENCES

[1] Kwon, Y.W. and J.E. Akin, *Development of a derivative singular element for application to crack propagation problems.* Computers & Structures, 1989. **31**(3): p. 467-471.
[2] Nash Gifford, L. and P.D. Hilton, *Stress intensity factors by enriched finite elements.* Engineering Fracture Mechanics, 1978. **10**(3): p. 485-496.
[3] Moës, N., J. Dolbow, and T. Belytschko, *A finite element method for crack growth without remeshing.* International Journal for Numerical Methods in Engineering, 1999. **46**(1): p. 131-150.
[4] Kumar, S., I.V. Singh, and B.K. Mishra, *A homogenized XFEM approach to simulate fatigue crack growth problems.* Computers & Structures, 2015. **150**(Supplement C): p. 1-22.

[5] Liu, P., et al., *The singular edge-based smoothed finite element method for stationary dynamic crack problems in 2D elastic solids.* Computer Methods in Applied Mechanics and Engineering, 2012. **233-236**(Supplement C): p. 68-80.
[6] Bui, T.Q., *Extended isogeometric dynamic and static fracture analysis for cracks in piezoelectric materials using NURBS.* Computer Methods in Applied Mechanics and Engineering, 2015. **295**(Supplement C): p. 470-509.
[7] Zheng, C., et al., *A novel twice-interpolation finite element method for solid mechanics problems.* Acta Mechanica Sinica, 2010. **26**(2): p. 265-278.
[8] Barsoum, R.S., *Application of quadratic isoparametric finite elements in linear fracture mechanics.* International Journal of Fracture, 1974. **10**(4): p. 603-605.
[9] Henshell, R.D. and K.G. Shaw, *Crack tip finite elements are unnecessary.* International Journal for Numerical Methods in Engineering, 1975. **9**(3): p. 495-507.
[10] Ewalds, H. and R. Wanhill, *Fracture Mechanics*. 1989, New York: Edward Arnold.
[11] Aliabadi, M.H., D.J. Cartwright, and D.P. Rooke, *Fracture-mechanics weight-functions by the removal of singular fields using boundary element analysis.* International Journal of Fracture, 1989. **40**(4): p. 271-284.
[12] Srawley, J.E., *Wide range stress intensity factor expressions for ASTM E 399 standard fracture toughness specimens.* International Journal of Fracture, 1976. **12**(3): p. 475-476.
[13] Kang, Z., et al., *An extended consecutive-interpolation quadrilateral element (XCQ4) applied to linear elastic fracture mechanics.* Acta Mechanica, 2015. **226**(12): p. 3991-4015.
[14] Wu, J. and Y. Cai, *A partition of unity formulation referring to the NMM for multiple intersecting crack analysis.* Theoretical and Applied Fracture Mechanics, 2014. **72**: p. 28-36.

Corresponding author:
Ton That Hoang Lan
Ho Chi Minh City University of Architecture
Email: hoanglantonthat@gmail.com / 1721001@student.hcmute.edu.vn